

Supporting Information

Charge effect in protein metalation reactions by diruthenium complexes

Aarón Terán,^a Giarita Ferraro,^b Ana E. Sánchez-Peláez,^a Santiago Herrero^{a*} and Antonello Merlino^{b*}

^aMatMoPol Research Group. Inorganic Chemistry Department, Faculty of Chemical Sciences, Complutense University of Madrid, Avda. Complutense s/n, E-28040 Madrid, Spain.

^bDepartment of Chemical Sciences, University of Naples Federico II, Complesso Universitario di Monte Sant'Angelo, via Cinthia, 21, 80126, Naples, Italy.

*E-mail: antonello.merlino@unina.it; sherrero@ucm.es

Index	
Materials	4
Synthesis	4
Scheme S1. Synthesis of $K_2[Ru_2(L-L)(CO_3)_3]$ compounds by the reaction of $[Ru_2Cl(L-L)(O_2CCH_3)_3]$ with K_2CO_3 in $H_2O:EtOH$ (1:21.4) solution at room temperature (L-L = D- <i>p</i> -FPhF ⁻ or DAniF ⁻).	4
Characterization	4
Crystallization, X-ray diffraction data collection, structure solution and refinement of the adducts with HEWL	6
Table S1. Estimated melting temperatures (T_m) of HEWL and HEWL in the presence of diruthenium compounds at 1:3 HEWL: Ru_2 molar ratio under different conditions.	7
Table S2. Data collection and refinement statistics.	8
Figure S1. FT-IR spectra of $K_2[Ru_2(D-p-FPhF)(CO_3)_3] \cdot 3H_2O \cdot EtOH$ (upper) and $K_2[Ru_2(DAniF)(CO_3)_3] \cdot 3H_2O$ (lower).	9
Figure S2. ESI mass peaks of $K_2[Ru_2(D-p-FPhF)(CO_3)_3] \cdot 3H_2O \cdot EtOH$ acquired in water (Molecular weight = 791.70 g/mol). Experimental (upper) and simulated (lower) isotopic distribution. $S = 3H_2O + EtOH$	10
Figure S3. ESI mass peaks of $K_2[Ru_2(DAniF)(CO_3)_3] \cdot 3H_2O$ acquired in water (Molecular weight = 769.70 g/mol). Experimental (upper) and simulated (lower) isotopic distribution. $S = 3H_2O$	11
Figure S4. Cyclic voltammograms for $[Ru_2Cl(O_2CCH_3)_4]$, $K_3[Ru_2(CO_3)_4]$, $[Ru_2Cl(L-L)(O_2CCH_3)_3]$ and $K_2[Ru_2(L-L)(CO_3)_3]$ (L-L = DAniF ⁻ or D- <i>p</i> -FPhF ⁻) derivatives. Experiments shown for 0.1 M KCl and scan rate = 100 mV/s.	12
Figure S5. UV-vis spectra of $K_3[Ru_2(CO_3)_4]$ (A), $K_2[Ru_2(D-p-FPhF)(CO_3)_3]$ (B), $K_2[Ru_2(DAniF)(CO_3)_3]$ (C), and $[Ru_2Cl(DAniF)(O_2CCH_3)_3]$ (D) in pure water recorded as a function of time during the incubation for 24h. Metal compound concentration = 500 μ M.	13
Figure S6. Time course UV-vis spectra of 500 μ M $K_3[Ru_2(CO_3)_4]$ in 20% ethylene glycol, 0.1 M sodium acetate buffer at pH 4.0, 0.6 M sodium nitrate in the absence (A) and in the presence (B) of HEWL and in 2.0 M sodium formate, 0.1 M HEPES buffer pH 7.5 in the absence (C) and in the presence (D) of HEWL.	14
Figure S7. Time course UV-vis spectra of 500 μ M $K_2[Ru_2(D-p-FPhF)(CO_3)_3]$ in 20% ethylene glycol, 0.1 M sodium acetate buffer at pH 4.0, 0.6 M sodium nitrate in the absence (A) and in the presence (B) of HEWL and in 2.0 M sodium formate, 0.1 M HEPES buffer pH 7.5 in the absence (C) and in the presence (D) of HEWL.	15
Figure S8. Time course UV-vis spectra of 500 μ M $[Ru_2Cl(DAniF)(O_2CCH_3)_3]$ in 20% ethylene glycol, 0.1 M sodium acetate buffer at pH 4.0, 0.6 M sodium nitrate in the absence (A) and in the presence (B) of HEWL and in 2.0 M sodium formate, 0.1 M HEPES buffer pH 7.5 in the absence (C) and in the presence (D) of HEWL.	16
Figure S9. Time course UV-vis spectra of 500 μ M $K_2[Ru_2(DAniF)(CO_3)_3]$ in 20% ethylene glycol, 0.1 M sodium acetate buffer at pH 4.0, 0.6 M sodium nitrate in the absence (A) and in the presence (B) of HEWL and in 2.0 M sodium formate, 0.1 M HEPES buffer pH 7.5 in the absence (C) and in the presence (D) of HEWL.	17
Figure S10. Fluorescence emission spectra of HEWL in (A-B) 10 mM sodium acetate buffer pH 4.0 and (C-D) 10 mM HEPES buffer pH 7.5 upon titration with a solution of $K_2[Ru_2(CO_3)_4]$. Spectra have been collected using $\lambda_{ex} = 280$ nm (panels A and C) and 295 nm (panels B and D).	18
Figure S11. Fluorescence emission spectra of HEWL in (A-B) 10 mM sodium acetate buffer pH 4.0 and (C-D) 10 mM HEPES buffer pH 7.5 upon titration with a solution of $K_2[Ru_2(D-p-FPhF)(CO_3)_3]$. Spectra have been collected using $\lambda_{ex} = 280$ nm (panels A and C) and 295 nm (panels B and D).	19

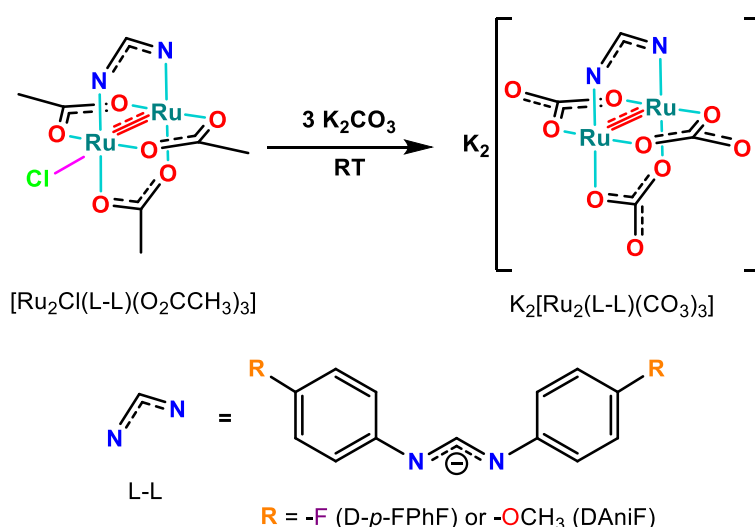
Figure S12. Fluorescence emission spectra of HEWL in (A-B) 10 mM sodium acetate buffer pH 4.0 and (C-D) 10 mM Hepes buffer pH 7.5 upon titration with a solution of [Ru₂Cl(DAniF)(O₂CCH₃)₃] . Spectra have been collected using $\lambda_{\text{ex}} = 280$ nm (panels A and C) and 295 nm (panels B and D).	20
Figure S13. Fluorescence emission spectra of HEWL in (A-B) 10 mM sodium acetate buffer pH 4.0 and (C-D) 10 mM Hepes buffer pH 7.5 upon titration with a solution of K₂[Ru₂(DAniF)(CO₃)₃] . Spectra have been collected using $\lambda_{\text{ex}} = 280$ nm (panels A and C) and 295 nm (panels B and D).	21
Figure S14. Far-UV CD spectra of HEWL (7.0 μ M concentration) incubated for 24 h in the presence of K₃[Ru₂(CO₃)₄] (A), K₂[Ru₂(D-<i>p</i>-FPhF)(CO₃)₃] (B), K₂[Ru₂(DAniF)(CO₃)₃] (C), and [Ru₂Cl(DAniF)(O₂CCH₃)₃] (D) in 10 mM sodium acetate buffer pH 4.0 in different protein to diruthenium molar ratios. CD spectrum of metal-free protein is in black.	22
Figure S15. Hepes molecule found in the structure of the adduct formed in the reaction between HEWL and K₂[Ru₂(D-<i>p</i>-FPhF)(CO₃)₃] in the condition B. $2F_{\sigma}-F_c$ electron density maps are contoured at 1.0 σ (grey) level.	23

Materials

All the reactions and manipulations were performed under air atmosphere. All reactants and solvents were obtained from commercial sources and used without further purification unless otherwise indicated. HEWL was purchased from Sigma Chemical Co (Merck Life Science S.r.l., Milan, Italy) at highest grade of purity.

Synthesis

The syntheses of $[\text{Ru}_2\text{Cl}(\text{O}_2\text{CCH}_3)_4]$,¹ $\text{K}_3[\text{Ru}_2(\text{CO}_3)_4]\cdot 4\text{H}_2\text{O}$,² $[\text{Ru}_2\text{Cl}(\text{D-}p\text{-FPhF})(\text{O}_2\text{CCH}_3)_3]$ ³ and $[\text{Ru}_2\text{Cl}(\text{DAniF})(\text{O}_2\text{CCH}_3)_3]$ ⁴ had been previously described. The HDAniF and HD-*p*-FPhF formamidines were prepared according to a published general procedure.⁵ $[\text{Ru}_2\text{Cl}(\text{D-}p\text{-FPhF})(\text{O}_2\text{CCH}_3)_3]$ and $[\text{Ru}_2\text{Cl}(\text{DAniF})(\text{O}_2\text{CCH}_3)_3]$ were used as starting material to prepare $\text{K}_2[\text{Ru}_2(\text{D-}p\text{-FPhF})(\text{CO}_3)_3]$ and $\text{K}_2[\text{Ru}_2(\text{DAniF})(\text{CO}_3)_3]$ compounds.



Scheme S1. Synthesis of $\text{K}_2[\text{Ru}_2(\text{L-L})(\text{CO}_3)_3]$ compounds by the reaction of $[\text{Ru}_2\text{Cl}(\text{L-L})(\text{O}_2\text{CCH}_3)_3]$ with K_2CO_3 in $\text{H}_2\text{O}:\text{EtOH}$ (1:21.4) solution at room temperature (L-L = D-*p*-FPhF or DAniF).

A mixture of a solution of the corresponding $[\text{Ru}_2\text{Cl}(\text{L-L})(\text{O}_2\text{CCH}_3)_3]$ (L-L = D-*p*-FPhF or DAniF) compound (0.1 mmol in 30 mL of EtOH) and a solution of K_2CO_3 (0.3 mmol in 1.4 mL of H_2O) was vigorously stirred overnight. The dark-orange solid formed was filtered, washed with EtOH (5×10 mL) and dried under vacuum to give analytically pure materials.

$\text{K}_2[\text{Ru}_2(\text{D-}p\text{-FPhF})(\text{CO}_3)_3]\cdot 3\text{H}_2\text{O}\cdot \text{EtOH}$: Yield: 95%. Elemental analysis found (calculated) for $\text{C}_{18}\text{H}_{21}\text{F}_2\text{K}_2\text{N}_2\text{O}_{13}\text{Ru}_2$ (MW = 791.70 g/mol): C, 27.11 (27.31); H, 2.57 (2.67); N, 3.76 (3.54). ATR-FT-IR: 1639, 1528, 1458, 1299, 1204, 1153, 1056, 947, 836, 780, 694 cm^{-1} . ESI (m/z): 675.0 $[\text{M} - 3\text{H}_2\text{O} - \text{EtOH} + \text{H}^+]^+$, 650.7 $[\text{M} - \text{K}^+ - 3\text{H}_2\text{O} - \text{EtOH} + 2\text{H}^+]^+$, 615.7 $[\text{M} - 2\text{K}^+ - 3\text{H}_2\text{O} - \text{EtOH} + 3\text{H}^+]^+$.

$\text{K}_2[\text{Ru}_2(\text{DAniF})(\text{CO}_3)_3]\cdot 3\text{H}_2\text{O}$: Yield: 99%. Elemental analysis found (calculated) for $\text{C}_{18}\text{H}_{21}\text{K}_2\text{N}_2\text{O}_{14}\text{Ru}_2$ (MW = 769.70 g/mol): C, 27.86 (28.09); H, 3.19 (2.75); N, 3.45 (3.64). ATR-FT-IR: 1646, 1529, 1444, 1294, 1216, 1170, 1031, 945, 829, 768, 694 cm^{-1} . ESI (m/z): 715.7 $[\text{M} - 3\text{H}_2\text{O} + \text{H}^+]^+$ and 671.7 $[\text{M} - \text{K}^+ - 3\text{H}_2\text{O} + 2\text{H}^+]^+$.

Characterization

FTIR spectra (4000–500 cm^{-1}) were recorded with a Perkin-Elmer Spectrum 100 with a universal ATR accessory. Elemental analyses were performed at the Microanalytical Service of the Universidad

Complutense de Madrid. Mass spectrometry data (electrospray ionization) were recorded at the Mass Spectrometry Service of the Universidad Complutense de Madrid, using an ion trap analyser HCT Ultra (Bruker Daltonics) mass spectrometer in water solution.

Cyclic voltammetry (CV) measurements were conducted with a Metrohm Autolab PGSTAT204 potentiostat. The working electrode was a glassy carbon electrode (GCE). A Pt wire served as the counter electrode and Ag/AgCl was employed as the reference electrode. Electrochemical grade KCl at a concentration of 0.10 M was employed as the supporting electrolyte in voltammetric measurements. High pure N₂ was used to deoxygenate the solution at least 10 minutes prior to each run and to maintain a nitrogen blanket. The ferrocenium/ferrocene couple was observed at 0.53 V (vs. Ag/AgCl) in 0.1 M tetrabutylammonium perchlorate (TBAP) dichloromethane solution.

UV-vis spectra of K₃[Ru₂(CO₃)₄], K₂[Ru₂(D-*p*-FPhF)(CO₃)₃], [Ru₂Cl(DAniF)(O₂CCH₃)₃] and K₂[Ru₂(DAniF)(CO₃)₃] were recorded on a Jasco V-750 spectrophotometer using quartz cuvette of 1 cm path length, a 50 μM diruthenium concentration in water and in other two different experimental conditions, i.e. those used to grow HEWL crystals: A) 20% ethylene glycol, 0.1 M sodium acetate buffer at pH 4.0, 0.6 M sodium nitrate; B) 2.0 M sodium formate, 0.1 M Hepes buffer pH 7.5. Spectra were collected for 5 hours continuously, and then after 24 hours and 7 days, in the absence and in the presence of HEWL (protein to metal compound molar ratio 1:3). Other experimental parameters were wavelength range 240–700 nm, data pitch 1.0 nm, scanning speed 400 nm/min, band width 2.0 nm. Each measurement was repeated twice.

Far **UV-CD** spectra were recorded on a Jasco J-715 spectropolarimeter equipped with a Peltier thermostatic cell holder (Model PTC-348WI) in the range of 200–250 nm, using a protein concentration of 7 μM and a quartz cell with 0.1 cm path length. HEWL was incubated 24 h with increasing amounts of K₃[Ru₂(CO₃)₄], K₂[Ru₂(D-*p*-FPhF)(CO₃)₃], [Ru₂Cl(DAniF)(O₂CCH₃)₃] and K₂[Ru₂(DAniF)(CO₃)₃] to obtain the following protein to diruthenium molar ratios: 1:0.1, 1:1, 1:2, 1:3. Spectra were collected in: 10 mM sodium acetate buffer at pH 4.0 and 10 mM Hepes buffer at pH 7.5. Other experimental parameters were 1.0 nm data pitch, 2.0 nm bandwidth, 50 nm/min scanning speed, 2.0 s response time, and 25 °C. Each spectrum was obtained by averaging three scans. **Thermal denaturation** experiments were performed by following the CD signal at 222 nm as a function of temperature for HEWL and the adducts formed upon reaction with the diruthenium compounds (1:3 protein:metal compound molar ratio) using 7 μM of protein at two different pH values, pH 7.5 (10 mM Hepes buffer) and pH 4.0 (10 mM sodium acetate buffer). A Peltier temperature controller was used to set up the temperature of the sample, with a slope of 1 °C per min.

A HORIBA Fluoromax-4 spectrofluorometer equipped with a thermostat bath and a 1 cm path length cuvette was used to register **fluorescence** spectra of HEWL in the absence and in the presence of K₃[Ru₂(CO₃)₄], K₂[Ru₂(D-*p*-FPhF)(CO₃)₃], [Ru₂Cl(DAniF)(O₂CCH₃)₃] and K₂[Ru₂(DAniF)(CO₃)₃] at 25°C. HEWL solutions at a concentration of 1.4 μM were titrated with a 2 mM Ru₂ compound solution. The protein was excited at 280 nm (to follow Tyr and Trp emission) and 295 nm (to follow Trp emission only) over a range of wavelengths between 295 and 450 nm and between 310 and 450 nm, for excitation at 280 and 295 nm, respectively. Different protein to metal molar ratios were reached upon titration: 1:0.2, 1:0.5, 1:1, 1:2, 1:4, 1:6, 1:8, 1:10. Solutions were stirred and equilibrated for 5 minutes before recording the spectra. The titrations were carried out in two different buffers: 10 mM sodium acetate buffer pH 4.0 and 10 mM Hepes buffer pH 7.5. When necessary, correction of the fluorescence spectra was employed to compensate the effects of the existing primary and/or secondary internal filter using the following equation:

$$F_{\text{corr}} = F_{\text{obs}} 10^{(A_{\text{ex}} + A_{\text{em}}) / 2}$$

where F_{corr} and F_{obs} are, respectively, the corrected and observed fluorescence intensities, while A_{ex} and A_{em} are the absorbance values, respectively, at the excitation and emission wavelengths.

Each measurement was repeated twice.

Crystallization, X-ray diffraction data collection, structure solution and refinement of the adducts with HEWL

Crystals of HEWL were grown by the hanging drop vapor diffusion method mixing 1 μL of protein solution (concentration 13 mg/mL) with an equal volume of the reservoir solution containing the following conditions: 20% ethylene glycol, 0.1 M sodium acetate at pH 4.0 (**condition A**), and 0.6 M sodium nitrate, B) 2.0 M sodium formate, 0.1 M HEPES buffer pH 7.5 (**condition B**). Crystals grew in few days. These crystals were then exposed to stabilizing solutions containing the mother liquors and a saturated solution of $\text{K}_3[\text{Ru}_2(\text{CO}_3)_4]$, $\text{K}_2[\text{Ru}_2(\text{D-}p\text{-FPhF})(\text{CO}_3)_3]$, $\text{K}_2[\text{Ru}_2(\text{DAniF})(\text{CO}_3)_3]$ and $[\text{Ru}_2\text{Cl}(\text{DAniF})(\text{O}_2\text{CCH}_3)_3]$ for a soaking time of 14 days.

Crystals of the adducts of the four compounds with HEWL were then soaked in the reservoir solution supplemented with 25% (v/v) glycerol for a few seconds, flash-cooled in liquid nitrogen and stored under cryogenic conditions until data collection. The crystals diffract X-ray in the resolution range of 1.46-1.03 \AA . X-ray diffraction data collections were carried out on Beamline XRD2 at Elettra synchrotron (Trieste, Italy),⁶ using a wavelength of 1.00 \AA and a cold nitrogen stream of 100 K. The total oscillation was 360° , with 1° per image, and the exposure time was 1 s per image. Data were processed and scaled using with the automated data-processing autoPROC pipeline. Data collection statistics are reported in Table S2.

The structures were solved by molecular replacement using Phaser⁷ with the coordinates of metal-free HEWL deposited under the PDB accession codes 193L⁸ as template. REFMAC5⁹ was used for the refinement and Coot¹⁰ for manual model editing. The Ru atom positions were identified using anomalous difference (ΔF_{ano}) and difference Fourier $F_o - F_c$ electron density maps calculated using the Collaborative Computational Project Number 4 (CCP4) suite.^{11,12} Ligand positions were restraints to guide geometry optimization. Pymol (www.pymol.org) was used to generate molecular graphic figures. Refinement statistics are given in Table S2.

Coordinates and structure factors of the adducts were validated using the Protein Data Bank validation server¹³ and deposited in the PDB (www.rcsb.org) as entries 8PFU (HEWL with $[\text{Ru}_2(\text{CO}_3)_4]^{3-}$ in the condition A), 8PFT (HEWL with $[\text{Ru}_2(\text{D-}p\text{-FPhF})(\text{CO}_3)_3]^{3-}$ in the condition A), 8PFX (HEWL with $[\text{Ru}_2(\text{D-}p\text{-FPhF})(\text{CO}_3)_3]^{3-}$ in the condition B), 8PFW (HEWL with $[\text{Ru}_2(\text{DAniF})(\text{CO}_3)_3]^{2-}$ in the condition A), 8PFY (HEWL with $[\text{Ru}_2(\text{DAniF})(\text{CO}_3)_3]^{2-}$ in the condition B) and 8PFV (HEWL with $[\text{Ru}_2(\text{DAniF})(\text{O}_2\text{CCH}_3)_3]^+$ in the condition A). The results were visualized with PyMOL (Schrödinger).¹⁴

Table S1. Estimated melting temperatures (T_m) of HEWL and HEWL in the presence of diruthenium compounds at 1:3 HEWL:Ru₂ molar ratio under different conditions.

Entry	Protein to metal compound molar ratio	T_m (°C)	
		10 mM Hepes buffer pH 7.5	10 mM sodium acetate buffer pH 4.0
HEWL	-	78 ± 1	80 ± 1
K ₃ [Ru ₂ (CO ₃) ₄]/HEWL	1:3	76 ± 1	79 ± 1
K ₂ [Ru ₂ (D-p-FPhF)(CO ₃) ₃]/HEWL	1:3	80 ± 1	80 ± 1
K ₂ [Ru ₂ (DAniF)(CO ₃) ₃]/HEWL	1:3	81 ± 1	82 ± 1
K ₂ [Ru ₂ (DAniF)(O ₂ CCH ₃) ₃]/HEWL	1:3	77 ± 1	81 ± 1

Table S2. Data collection and refinement statistics.

Compound	HEWL + [Ru ₂ (CO ₃) ₄] ³⁻	HEWL + [Ru ₂ (D- <i>p</i> -FPhF)(CO ₃) ₃] ²⁻	HEWL + [Ru ₂ (DAniF)(CO ₃) ₃] ²⁻	HEWL + [Ru ₂ (DAniF)(O ₂ CCH ₃) ₃] ⁺	HEWL + [Ru ₂ (D- <i>p</i> -FPhF)(CO ₃) ₃] ²⁻	HEWL + [Ru ₂ (DAniF)(CO ₃) ₃] ²⁻
PDB code	8PFU	8PFT	8PFW	8PFV	8PFX	8PFY
Crystallization conditions			Condition A			Condition B
Soaking time			2 weeks			2 weeks
Data collection						
Space group	<i>P</i> 4 ₁ 2 ₁ 2	<i>P</i> 4 ₁ 2 ₁ 2	<i>P</i> 4 ₁ 2 ₁ 2	<i>P</i> 4 ₁ 2 ₁ 2	<i>P</i> 4 ₁ 2 ₁ 2	<i>P</i> 4 ₁ 2 ₁ 2
<i>a</i> (Å)	78.06	77.75	77.81	78.35	76.72	76.62
<i>b</i> (Å)	78.06	77.75	77.81	78.35	76.72	76.62
<i>c</i> (Å)	37.47	37.34	37.39	37.64	38.39	37.08
$\alpha/\beta/\gamma$ (°)	90.0/90.0/90.0	90.0/90.0/90.0	90.0/90.0/90.0	90.0/90.0/90.0	90.0/90.0/90.0	90.0/90.0/90.0
Molecules for asymmetric unit	1	1	1	1	1	1
Resolution range (Å)	55.20-1.18 (1.20-1.18)	54.98-1.42 (1.44-1.42)	55.02-1.12 (1.14-1.12)	55.40-1.46 (1.48-1.46)	38.36-1.03 (1.04-1.03)	54.18-1.19 (1.21-1.19)
Observations	858346 (21017)	281127 (14230)	917971 (37961)	217102 (9627)	654453 (16800)	750551 (22007)
Unique reflections	38622 (1683)	22171 (1093)	44515 (2171)	21101 (1035)	57486 (2835)	36175 (1773)
Completeness (%)	99.2 (88.6)	99.8 (100.0)	99.9 (100.0)	99.9 (100.0)	100.0 (99.9)	100.0 (100.0)
Redundancy	22.2 (12.5)	12.7 (13.0)	11.0 (9.1)	10.3 (9.3)	11.4 (5.9)	20.7 (12.4)
Rmerge (%)	0.034 (1.003)	0.048 (1.273)	0.054 (1.324)	0.047 (0.997)	0.034 (0.753)	0.131 (1.106)
Average <i>I</i> / σ (<i>I</i>)	42.5 (2.3)	24.0 (2.2)	27.2 (2.2)	23.7 (2.2)	33.7 (2.3)	14.4 (2.4)
CC _{1/2}	1.000 (0.750)	1.000 (0.833)	0.999 (0.807)	1.000 (0.762)	1.000 (0.858)	0.997 (0.843)
Anom. completeness (%)	99.2 (88.6)	99.9 (100.0)	100.0 (100.0)	100.0 (100.0)	99.8 (98.3)	100.0 (100.0)
Anom. Multiplicity	11.8 (6.5)	6.8 (6.8)	11.0 (9.1)	5.5 (4.9)	6.0 (3.1)	11.0 (6.4)
Refinement						
Resolution (Å)	1.18	1.30	1.12	1.46	1.03	1.19
N° reflections	36163	24331	42224	19847	52328	34188
N° reflections in working set	2199	359	2946	1445	2721	2491
<i>R</i> _{factor} / <i>R</i> _{free}	0.179/0.202	0.205/0.245	0.203/0.239	0.181/0.211	0.193/0.214	0.195/0.212
N° non-H atoms in the refin.	1275	1208	1252	1171	1254	1128
Average <i>B</i> -factors (Å ²)						
All atoms	16.8	26.2	17.8	23.6	12.3	15.9
Ru atoms	63.6/42.8 40.2/40.6 36.0/36.1 31.3/28.6 0.40/0.40	37.8/33.3 27.5/29.4	9.9/10.9 12.1/12.0 12.3/12.7	15.9/16.7	15.4/14.4 15.5/14.5 16.1/17.9	30.4
Ru occupancy	0.20/0.20 0.20/0.20 0.20/0.20	0.35/0.35 0.35/0.35	0.45/0.45 0.50/0.50 0.35/0.35	0.35/0.35	0.35/0.35 0.20/0.20 0.20/0.20	0.30
Ramachandran statistics						
Most favoured	96 (95.05%)	113 (95.76%)	107 (95.54%)	111 (93.28%)	108 (93.91%)	115 (95.04%)
Outliers	0	0	0	0	0	0
Rmsd bonds (Å)	0.013	0.010	0.011	0.013	0.013	0.012
Rmsd angles (°)	1.827	2.525	3.691	1.996	1.933	1.827

$$\dagger R_{\text{merge}} = \sum h \sum i |I(h,i) - \langle I(h) \rangle| / \sum h \sum i I(h,i)$$

where $I(h,i)$ is the intensity of the i^{th} measurement of reflection h and $\langle I(h) \rangle$ is the mean value of the intensity of reflection h

Condition A: 20% ethylene glycol, 0.6 M NaNO₃, 0.1 M sodium acetate pH 4.0

Condition B: 2 M sodium formate and 0.1 M Hepes, pH 7.5

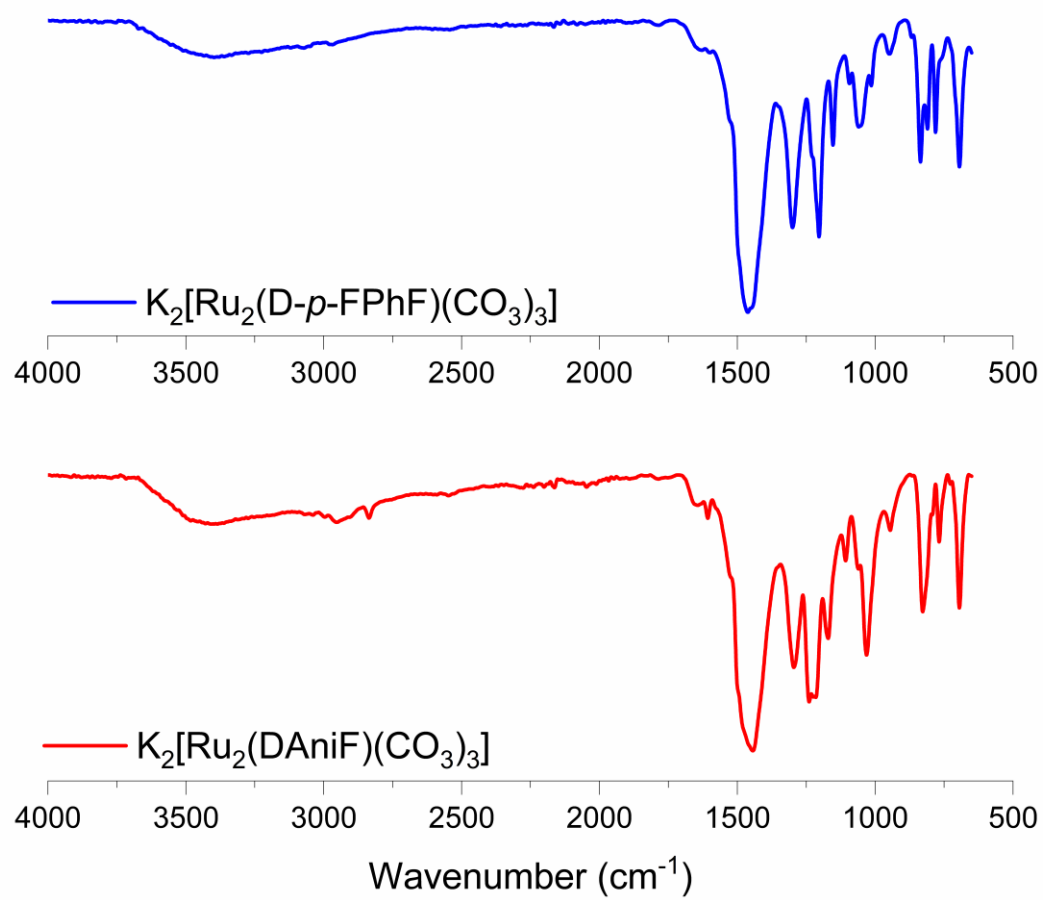


Figure S1. FT-IR spectra of $K_2[Ru_2(D-p-FPhF)(CO_3)_3] \cdot 3H_2O \cdot EtOH$ (upper) and $K_2[Ru_2(DAniF)(CO_3)_3] \cdot 3H_2O$ (lower).

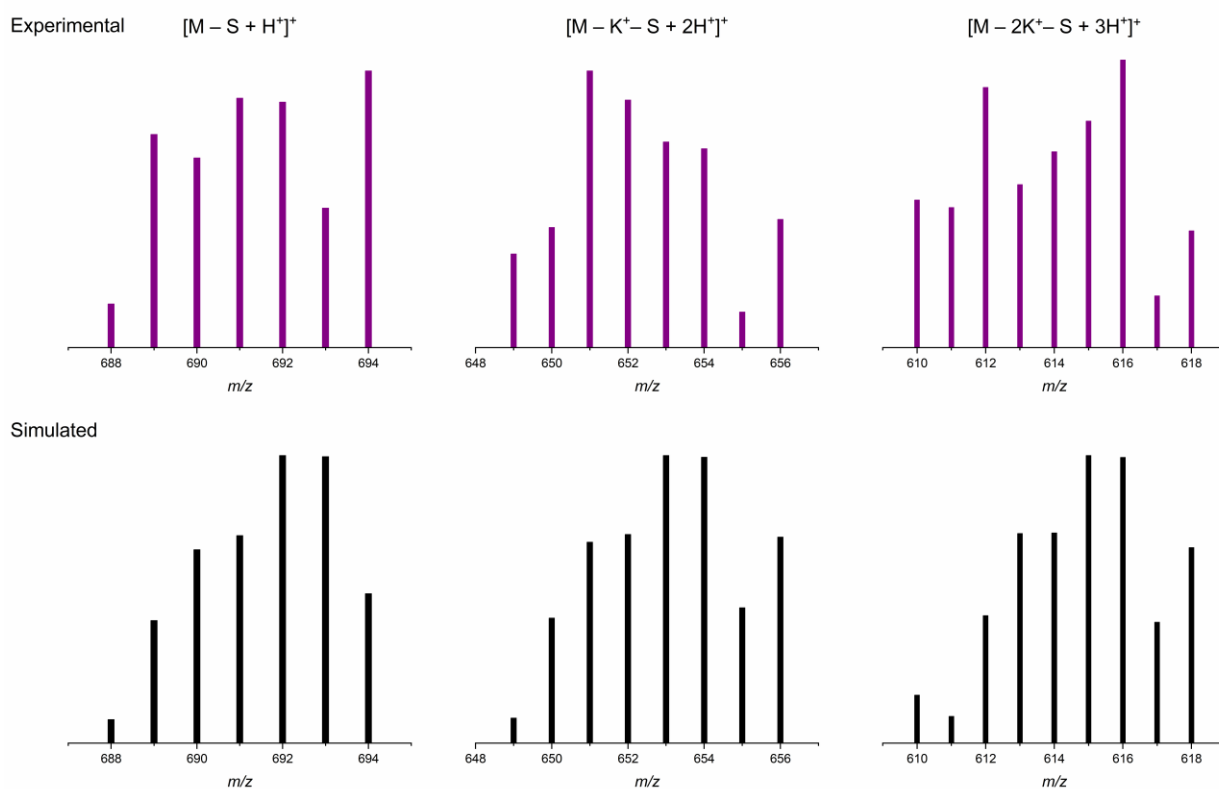
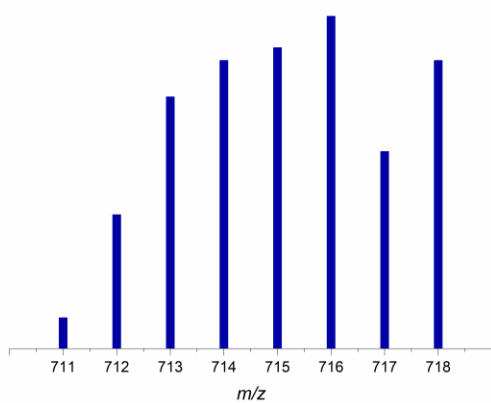


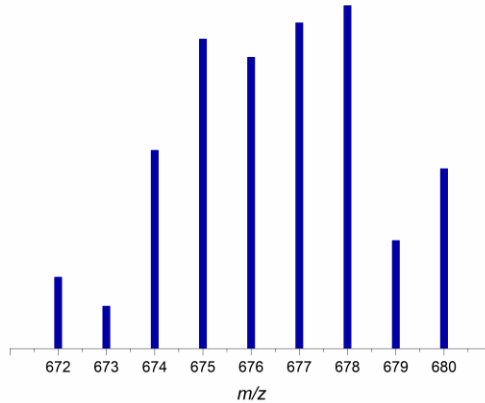
Figure S2. ESI mass peaks of $\text{K}_2[\text{Ru}_2(\text{D-}p\text{-FPhF})(\text{CO}_3)_3] \cdot 3\text{H}_2\text{O} \cdot \text{EtOH}$ acquired in water (Molecular weight = 791.70 g/mol). Experimental (upper) and simulated (lower) isotopic distribution. $\text{S} = 3\text{H}_2\text{O} + \text{EtOH}$.

Experimental

$[M - S + H^+]^+$



$[M - K^+ - S + 2H^+]^+$



Simulated

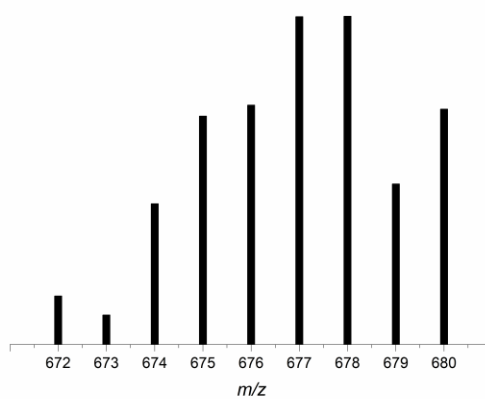
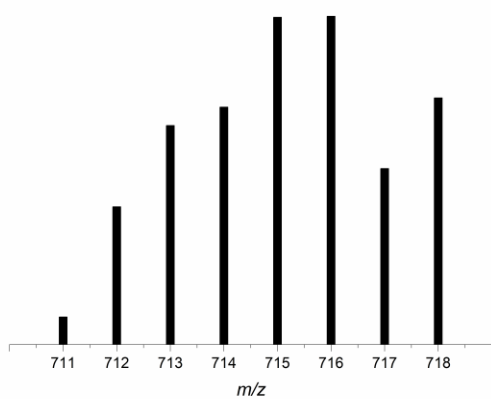


Figure S3. ESI mass peaks of $K_2[Ru_2(DAniF)(CO_3)_3] \cdot 3H_2O$ acquired in water (Molecular weight = 769.70 g/mol). Experimental (upper) and simulated (lower) isotopic distribution. $S = 3H_2O$.

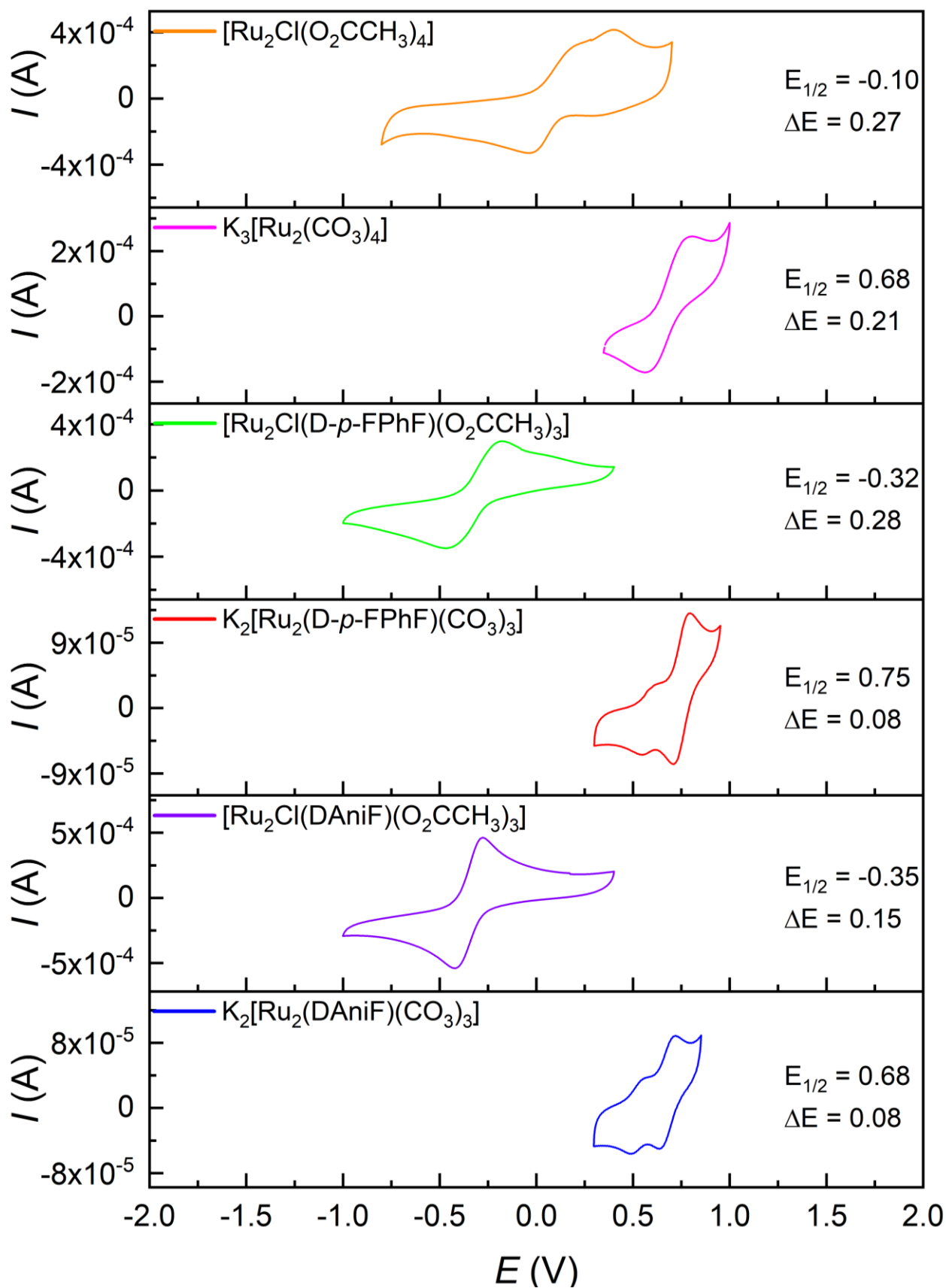


Figure S4. Cyclic voltammograms for $[\text{Ru}_2\text{Cl}(\text{O}_2\text{CCH}_3)_4]$, $\text{K}_3[\text{Ru}_2(\text{CO}_3)_4]$, $[\text{Ru}_2\text{Cl}(\text{L-L})(\text{O}_2\text{CCH}_3)_3]$ and $\text{K}_2[\text{Ru}_2(\text{L-L})(\text{CO}_3)_3]$ (L-L = DAniF⁻ or D-*p*-FPhF⁻) derivatives. Experiments shown for 0.1 M KCl and scan rate = 100 mV/s.

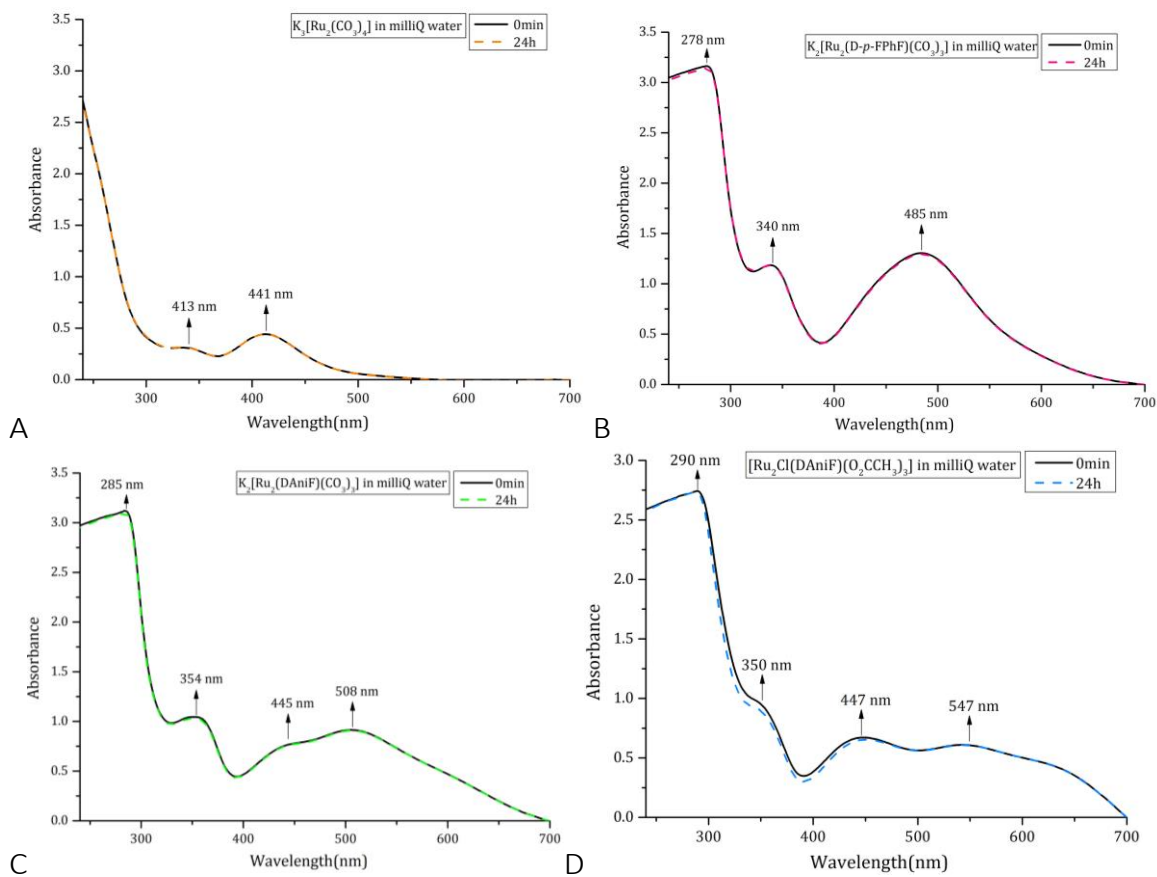


Figure S5. UV-vis spectra of $\text{K}_3[\text{Ru}_2(\text{CO}_3)_4]$ (A), $\text{K}_2[\text{Ru}_2(\text{D-}p\text{-FPhF})(\text{CO}_3)_3]$ (B), $\text{K}_2[\text{Ru}_2(\text{DAniF})(\text{CO}_3)_3]$ (C), and $[\text{Ru}_2\text{Cl}(\text{DAniF})(\text{O}_2\text{CCH}_3)_3]$ (D) in pure water recorded as a function of time during the incubation for 24h. Metal compound concentration = 500 μM .

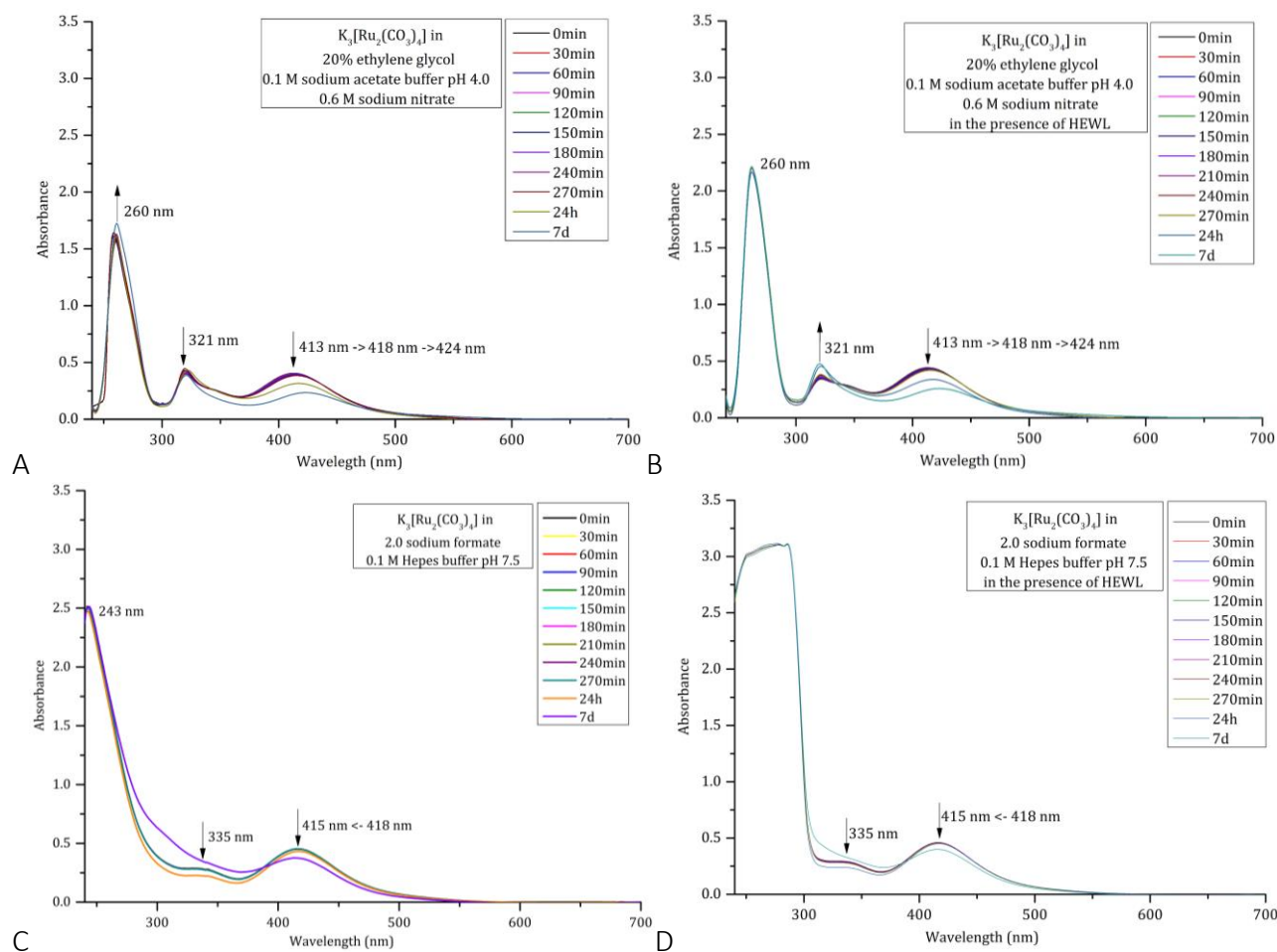


Figure S6. Time course UV-vis spectra of 500 μM $\text{K}_3[\text{Ru}_2(\text{CO}_3)_4]$ in 20% ethylene glycol, 0.1 M sodium acetate buffer at pH 4.0, 0.6 M sodium nitrate in the absence (A) and in the presence (B) of HEWL and in 2.0 M sodium formate, 0.1 M HEPES buffer pH 7.5 in the absence (C) and in the presence (D) of HEWL.

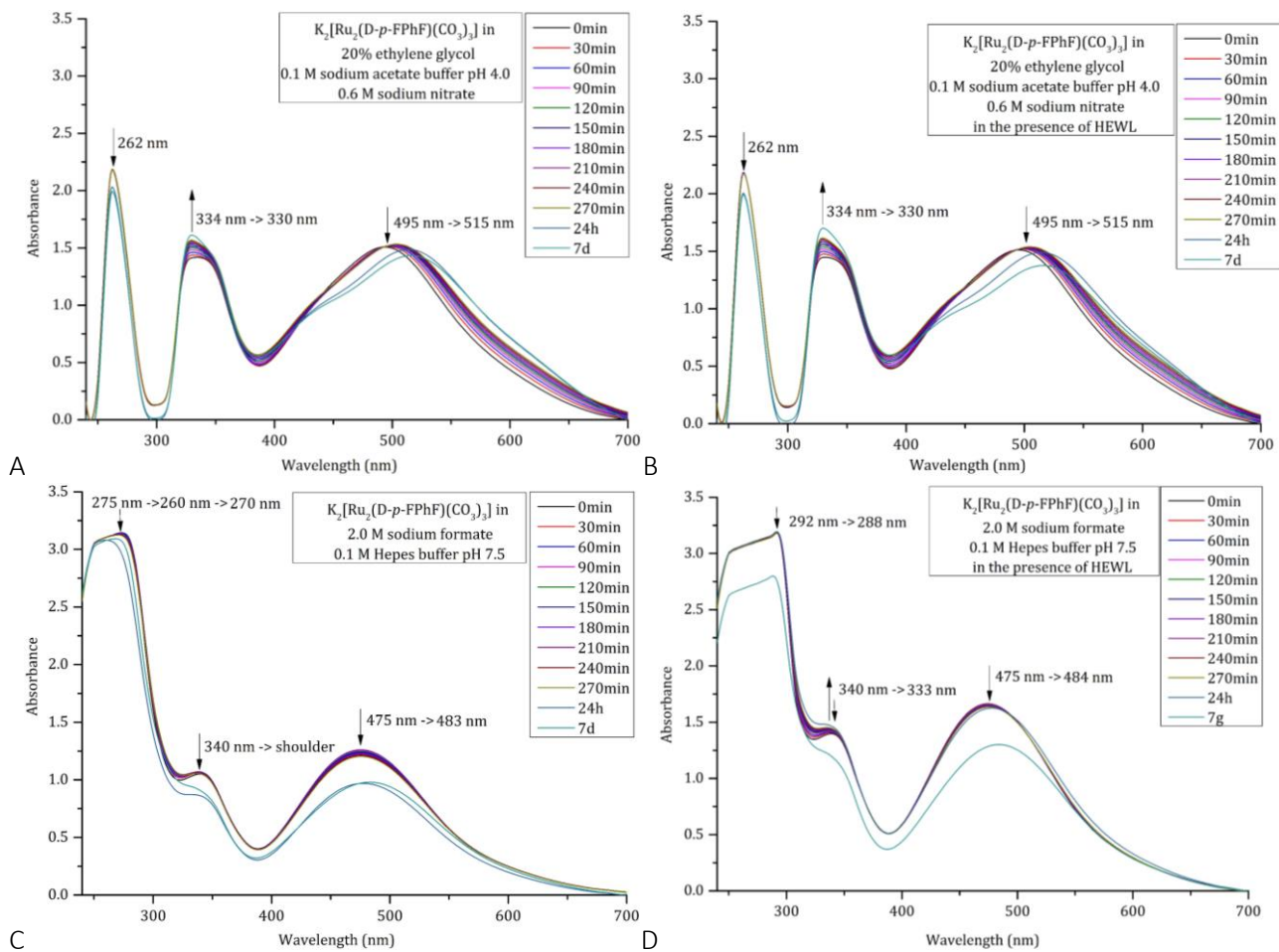


Figure S7. Time course UV-vis spectra of 500 μM $\text{K}_2[\text{Ru}_2(\text{D-}p\text{-FPhF})(\text{CO}_3)_3]$ in 20% ethylene glycol, 0.1 M sodium acetate buffer at pH 4.0, 0.6 M sodium nitrate in the absence (A) and in the presence (B) of HEWL and in 2.0 M sodium formate, 0.1 M HEPES buffer pH 7.5 in the absence (C) and in the presence (D) of HEWL.

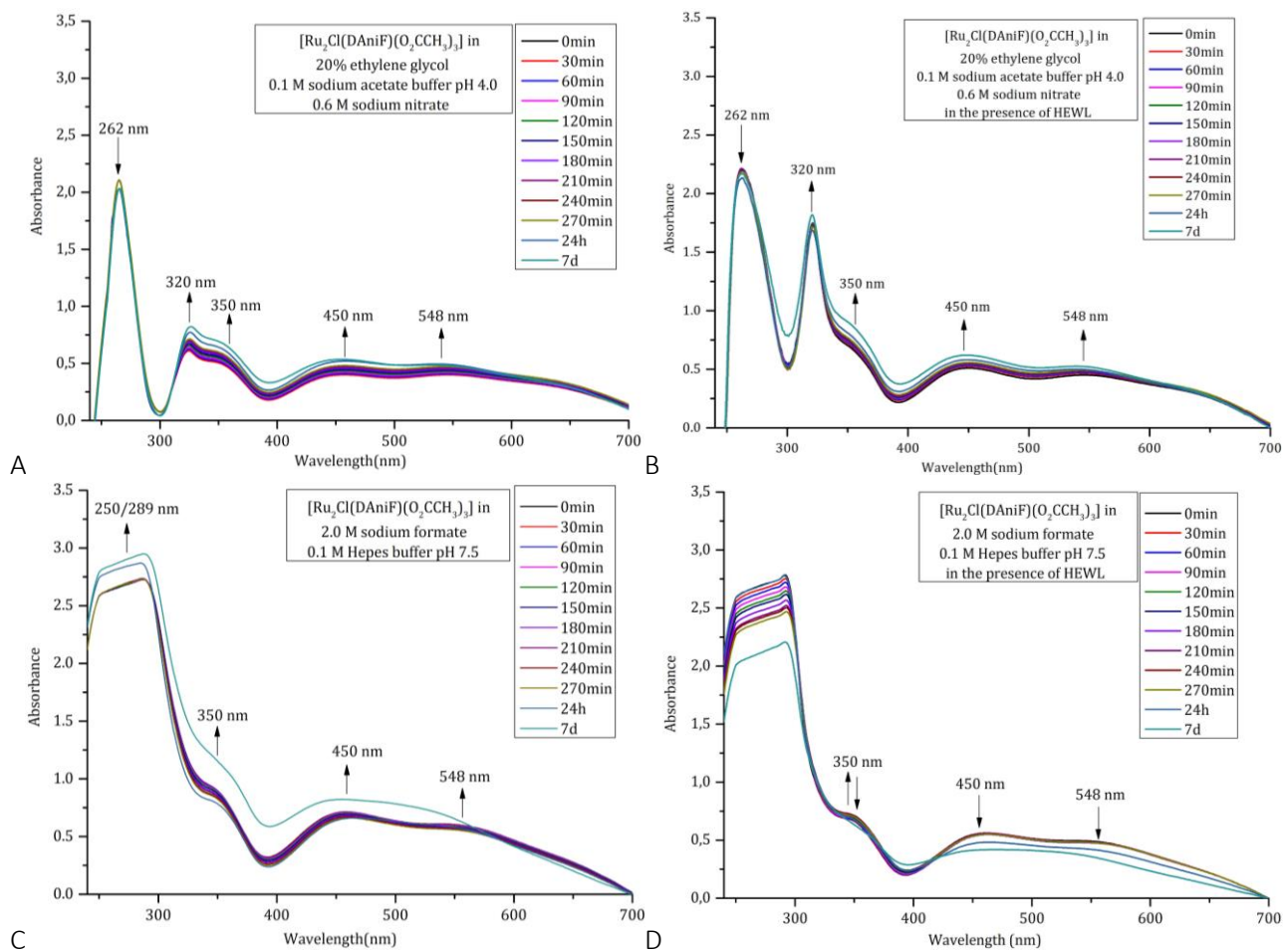


Figure S8. Time course UV-vis spectra of 500 μM $[\text{Ru}_2\text{Cl}(\text{DAniF})(\text{O}_2\text{CCH}_3)_3]$ in 20% ethylene glycol, 0.1 M sodium acetate buffer at pH 4.0, 0.6 M sodium nitrate in the absence (A) and in the presence (B) of HEWL and in 2.0 M sodium formate, 0.1 M HEPES buffer pH 7.5 in the absence (C) and in the presence (D) of HEWL.

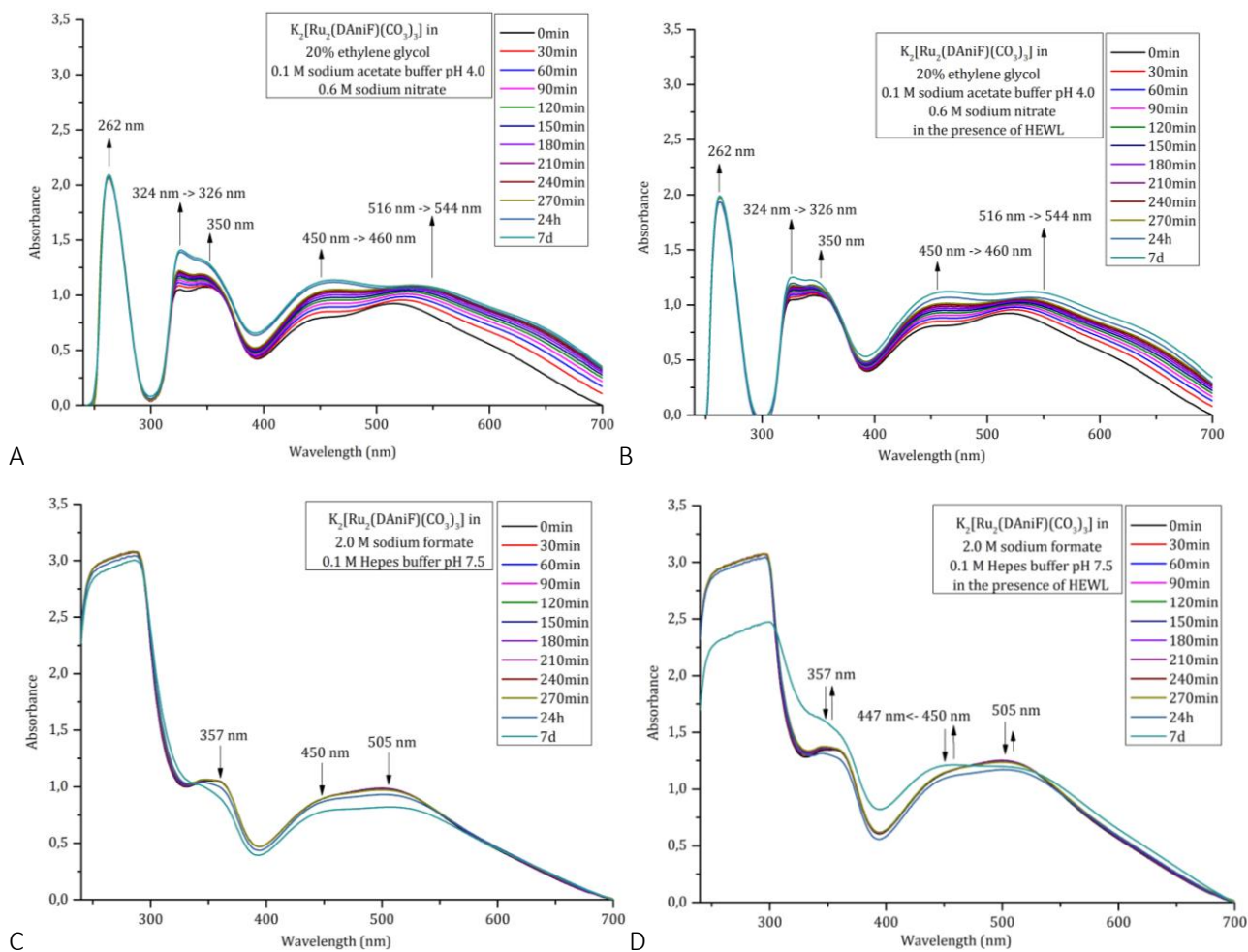


Figure S9. Time course UV-vis spectra of 500 μM $\text{K}_2[\text{Ru}_2(\text{DAniF})(\text{CO}_3)_3]$ in 20% ethylene glycol, 0.1 M sodium acetate buffer at pH 4.0, 0.6 M sodium nitrate in the absence (A) and in the presence (B) of HEWL and in 2.0 M sodium formate, 0.1 M HEPES buffer pH 7.5 in the absence (C) and in the presence (D) of HEWL.

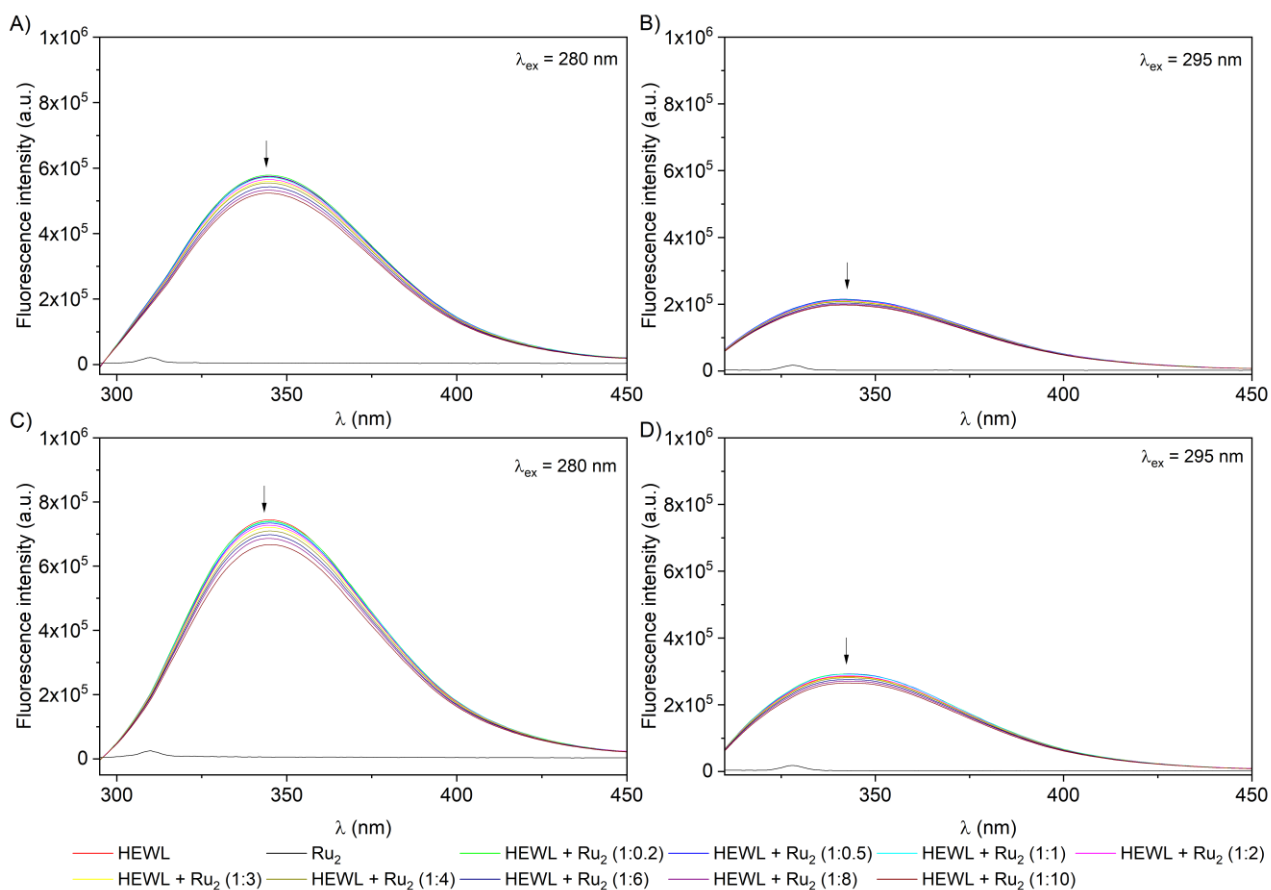


Figure S10. Fluorescence emission spectra of HEWL in (A-B) 10 mM sodium acetate buffer pH 4.0 and (C-D) 10 mM Hepes buffer pH 7.5 upon titration with a solution of $K_2[Ru_2(CO_3)_4]$. Spectra have been collected using $\lambda_{ex} = 280$ nm (panels A and C) and 295 nm (panels B and D).

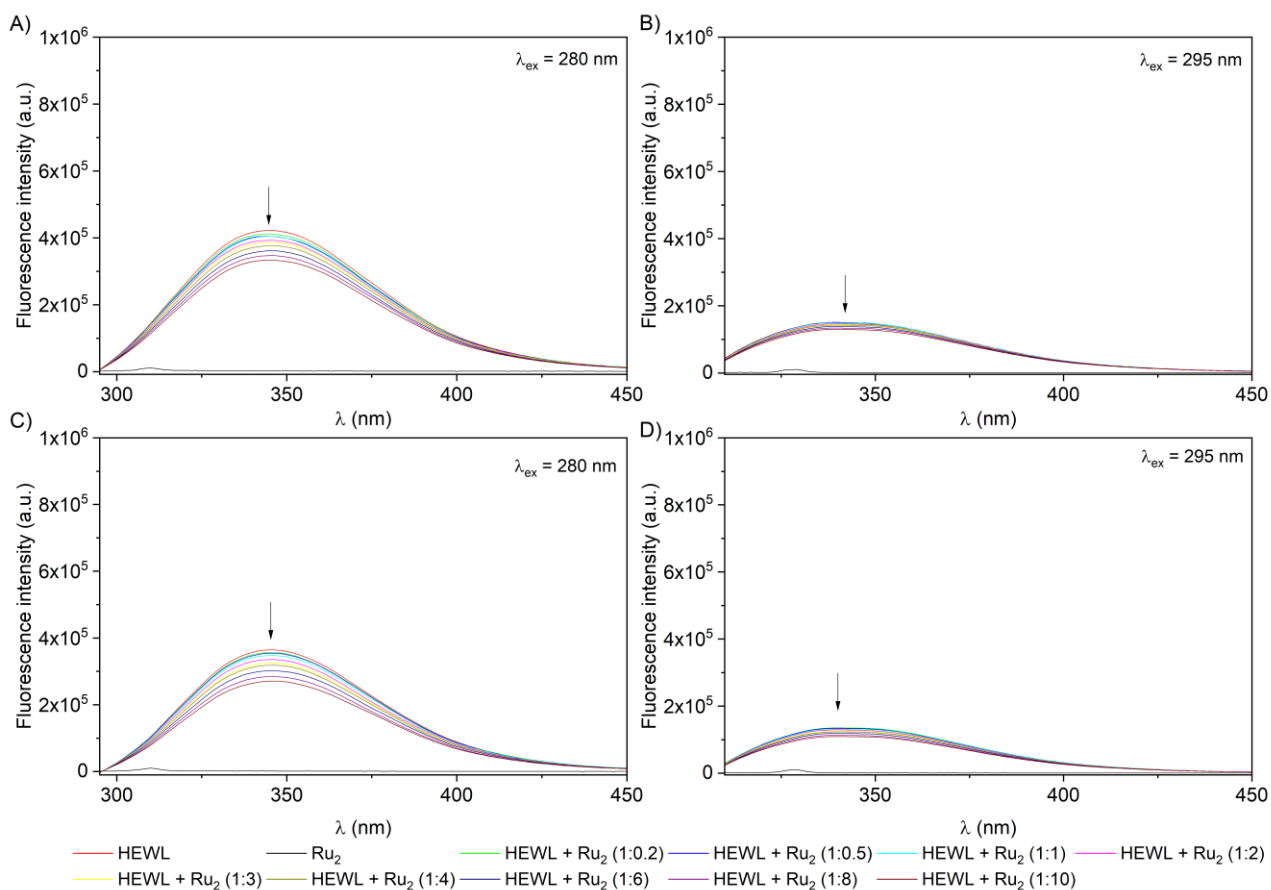


Figure S11. Fluorescence emission spectra of HEWL in (A-B) 10 mM sodium acetate buffer pH 4.0 and (C-D) 10 mM HEPES buffer pH 7.5 upon titration with a solution of $K_2[Ru_2(D-p-FPhF)(CO_3)_3]$. Spectra have been collected using $\lambda_{ex} = 280$ nm (panels A and C) and 295 nm (panels B and D).

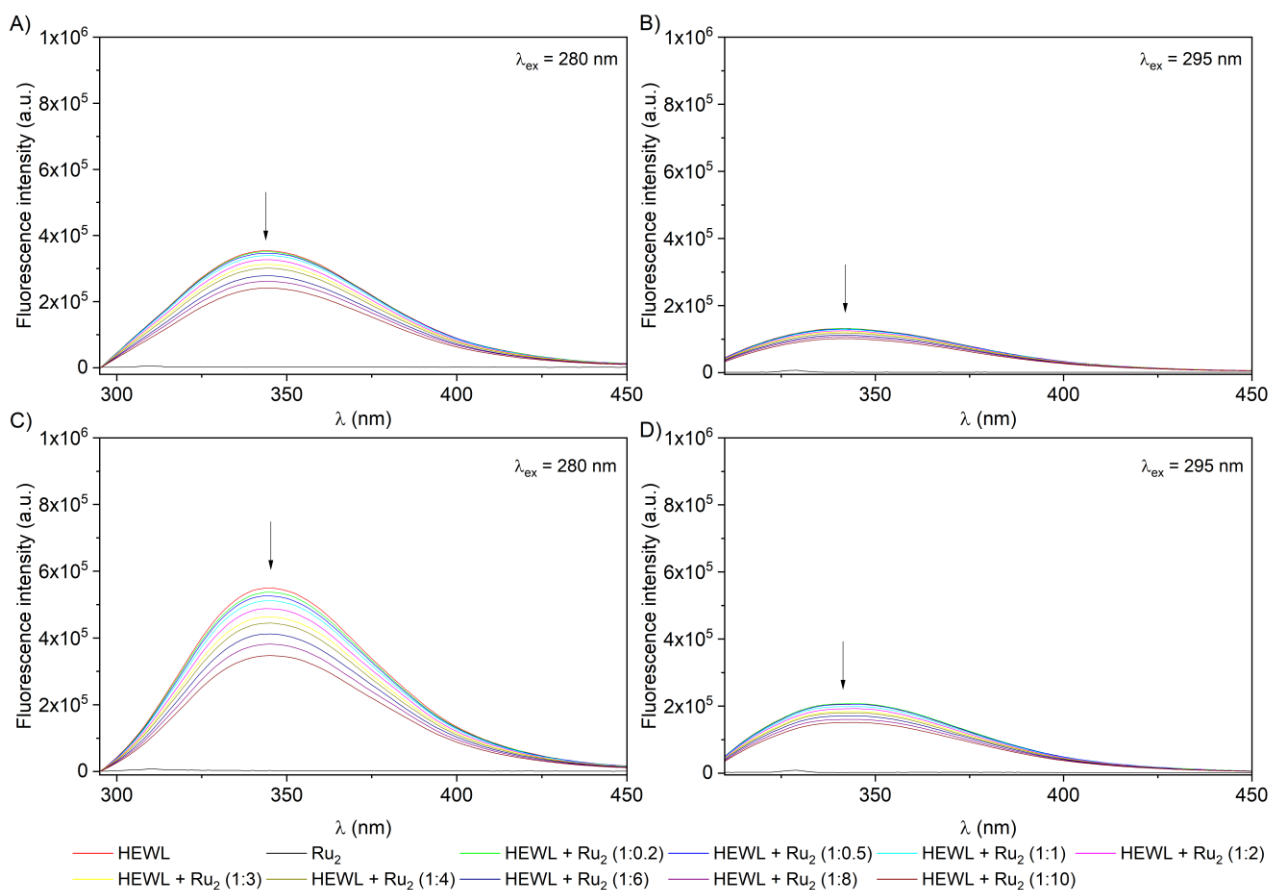


Figure S12. Fluorescence emission spectra of HEWL in (A-B) 10 mM sodium acetate buffer pH 4.0 and (C-D) 10 mM Hepes buffer pH 7.5 upon titration with a solution of $[\text{Ru}_2\text{Cl}(\text{DAniF})(\text{O}_2\text{CCH}_3)_3]$. Spectra have been collected using $\lambda_{\text{ex}} = 280$ nm (panels A and C) and 295 nm (panels B and D).

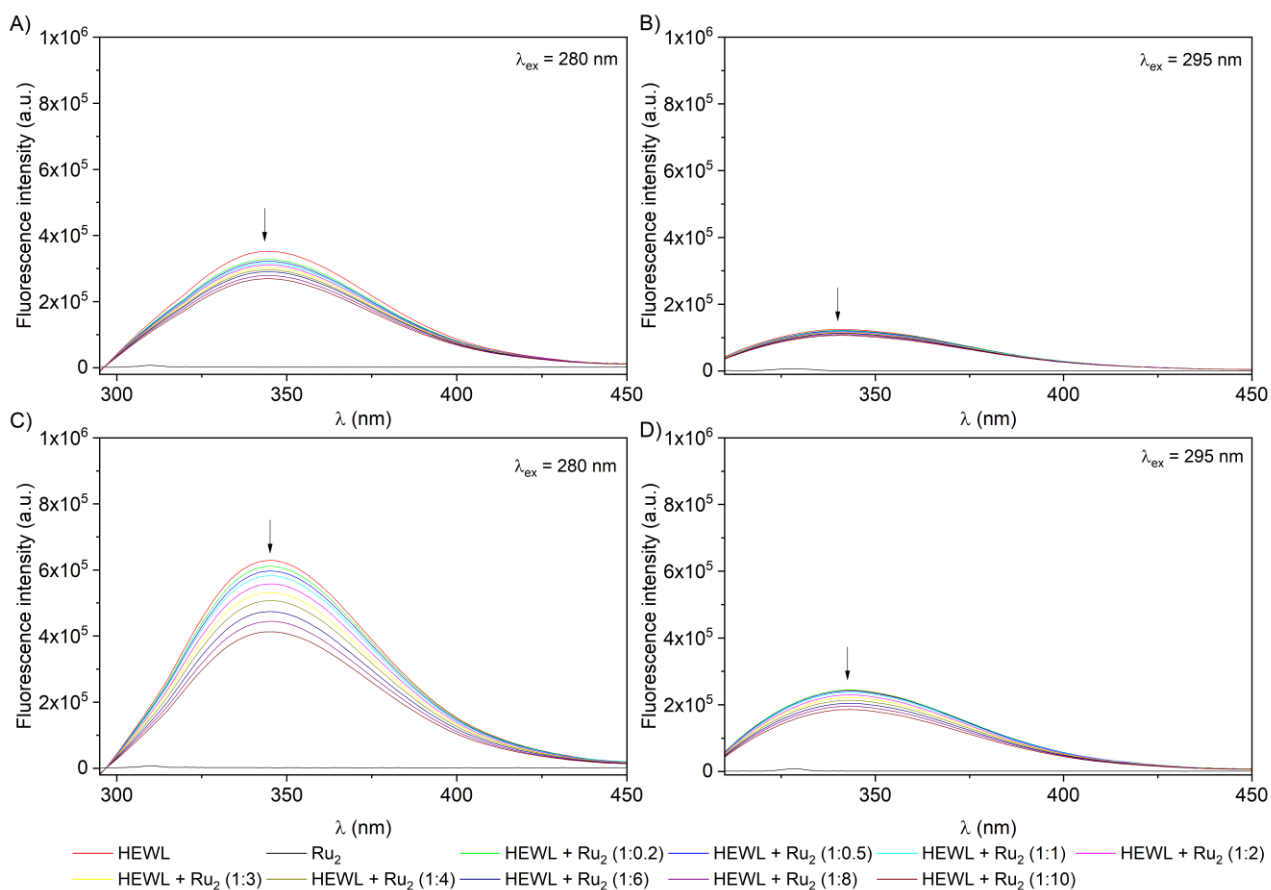


Figure S13. Fluorescence emission spectra of HEWL in (A-B) 10 mM sodium acetate buffer pH 4.0 and (C-D) 10 mM Hepes buffer pH 7.5 upon titration with a solution of $K_2[Ru_2(DAniF)(CO_3)_3]$. Spectra have been collected using $\lambda_{ex} = 280$ nm (panels A and C) and 295 nm (panels B and D).

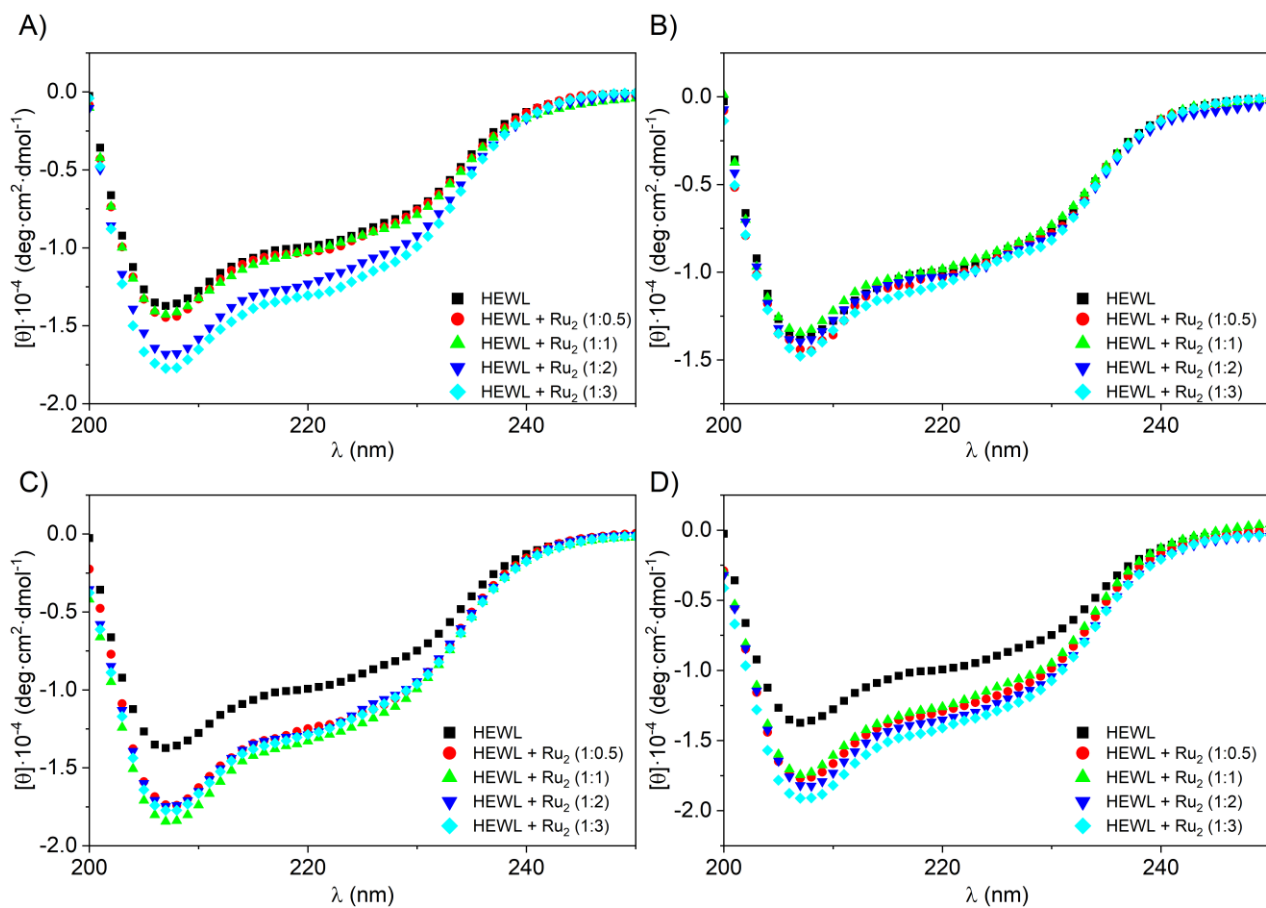


Figure S14. Far-UV CD spectra of HEWL (7.0 μ M concentration) incubated for 24 h in the presence of $K_3[Ru_2(CO_3)_4]$ (A), $K_2[Ru_2(D-p-FPhF)(CO_3)_3]$ (B), $K_2[Ru_2(DAniF)(CO_3)_3]$ (C), and $[Ru_2Cl(DAniF)(O_2CCH_3)_3]$ (D) in 10 mM sodium acetate buffer pH 4.0 in different protein to diruthenium molar ratios. CD spectrum of metal-free protein is in black.

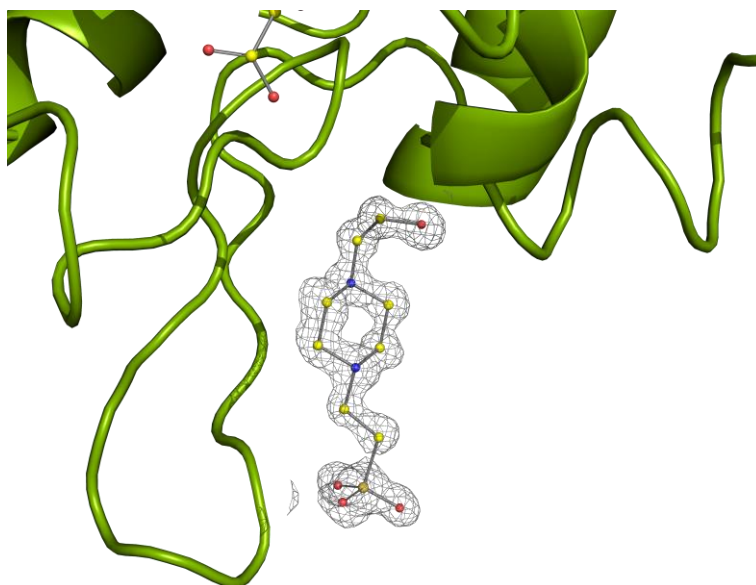


Figure S15. Hemes molecule found in the structure of the adduct formed in the reaction between HEWL and $\text{K}_2[\text{Ru}_2(\text{D-}p\text{-FPhF})(\text{CO}_3)_3]$ in the condition B. $2F_o-F_c$ electron density maps are contoured at 1.0σ (grey) level.

REFERENCES

- 1 R. W. Mitchell, A. Spencer and G. Wilkinson, *J. Chem. Soc., Dalton Trans.*, 1973, 846–854.
- 2 F. A. Cotton, L. Labella and M. Shang, *Inorg. Chem.*, 1992, **31**, 2385–2389.
- 3 A. Inchausti, A. Terán, A. Manchado-Parra, A. de Marcos-Galán, J. Perles, M. Cortijo, R. González-Prieto, S. Herrero and R. Jiménez-Aparicio, *Dalton Trans.*, 2022, **51**, 9708–9719.
- 4 A. Terán, M. Cortijo, Á. Gutiérrez, A. E. Sánchez-Peláez, S. Herrero and R. Jiménez-Aparicio, *Ultrason. Sonochem.*, 2021, **80**, 105828.
- 5 R. M. Roberts, *J. Org. Chem.*, 1949, **14**, 277–284.
- 6 A. Lausi, M. Polentarutti, S. Onesti, J. R. Plaisier, E. Busetto, G. Bais, L. Barba, A. Cassetta, G. Campi, D. Lamba, A. Pifferi, S. C. Mande, D. D. Sarma, S. M. Sharma and G. Paolucci, *Eur. Phys. J. Plus*, 2015, **130**, 43.
- 7 A. J. McCoy, R. W. Grosse-Kunstleve, P. D. Adams, M. D. Winn, L. C. Storoni and R. J. Read, *J. Appl. Crystallogr.*, 2007, **40**, 658–674.
- 8 M. C. Vaney, S. Maignan, M. Riès-Kautt and A. Ducruix, *Acta Crystallogr. D Biol. Crystallogr.*, 1996, **52**, 505–517.
- 9 G. N. Murshudov, A. A. Vagin and E. J. Dodson, *Acta Crystallogr. D Biol. Crystallogr.*, 1997, **53**, 240–255.
- 10 P. Emsley, B. Lohkamp, W. G. Scott and K. Cowtan, *Acta Crystallogr. D Biol. Crystallogr.*, 2010, **66**, 486–501.
- 11 E. Potterton, P. Briggs, M. Turkenburg and E. Dodson, *Acta Crystallogr. D Biol. Crystallogr.*, 2003, **59**, 1131–1137.
- 12 M. D. Winn, C. C. Ballard, K. D. Cowtan, E. J. Dodson, P. Emsley, P. R. Evans, R. M. Keegan, E. B. Krissinel, A. G. W. Leslie, A. McCoy, S. J. McNicholas, G. N. Murshudov, N. S. Pannu, E. A. Potterton, H. R. Powell, R. J. Read, A. Vagin and K. S. Wilson, *Acta Crystallogr. D Biol. Crystallogr.*, 2011, **67**, 235–242.
- 13 H. Berman, K. Henrick and H. Nakamura, *Nat. Struct. Mol. Biol.*, 2003, **10**, 980–980.
- 14 The PyMOL Molecular Graphics System, Version 2.0 Schrödinger, LLC.